ESMO GOOD SCIENCE BETTER MEDICINE BEST PRACTICE

ESMO OPEN CANCER HORIZONS

ORIGINAL RESEARCH

Long-term benefit of lurbinectedin as palliative chemotherapy in progressive malignant pleural mesothelioma (MPM): final efficacy and translational data of the SAKK 17/16 study

M. Mark[1*], S. Rusakiewicz[2,3,4], M. Früh[5,6,7], S. Hayoz[8], F. Grosso[9], M. Pless[10], P. Zucali[11,12], G. L. Ceresoli[13], A. Maconi[14], M. Schneider[8], P. Froesch[15], D. Tarussio[2,3,4], F. Benedetti[2,3,4], J. Dagher[16], L. Kandalaft[2,3,4], R. von Moos[1], S. Tissot-Renaud[2,3,4], S. Schmid[5,6] & Y. Metaxas[17]

[1]Department of Oncology/Haematology, Kantonsspital Graubünden, Chur; [2]Center of Experimental Therapeutics, Department of Oncology UNIL CHUV, Lausanne University Hospital, Lausanne; [3]Ludwig Institute for Cancer Research, Lausanne Branch, Lausanne; [4]Department of Oncology, UNIL CHUV, Lausanne University Hospital, Lausanne; [5]Department of Medical Oncology and Haematology, St. Gallen; [6]University of Bern, Bern; [7]Department of Medical Oncology, University of Bern, Bern; [8]SAKK Coordinating Centre, Bern, Switzerland; [9]Mesothelioma Unit e Oncology, SS. Antonio and C. Arrigo Hospital, Alessandria, Italy; [10]Department of Medical Oncology and Haematology, Kantonsspital Winterthur, Winterthur, Switzerland; [11]Department of Biomedical Sciences, Humanitas University, Milan; [12]Department of Oncology, IRCCS Humanitas Research Hospital, Milan; [13]Oncology Unit, Humanitas Gavazzeni Clinic, Bergamo; [14]Research Training Innovation Infrastructure, Research Innovation Department, Azienda Ospedaliera "SS Antonio e Biagio e Cesare Arrigo", Alessandria, Italy; [15]Oncology Institute of Southern Switzerland, Bellinzona; [16]Institute of Pathology, Lausanne University Hospital, Lausanne; [17]Department of Haematology and Oncology, Kantonsspital Münsterlingen, Münsterlingen, Switzerland

Available online xxx

Background: The SAKK 17/16 study showed promising efficacy data with lurbinectedin as second- or third-line palliative therapy in malignant pleural mesothelioma. Here, we evaluated long-term outcome and analyzed the impact of lurbinectedin monotherapy on the tumor microenvironment at the cellular and molecular level to predict outcomes.

Material and methods: Forty-two patients were treated with lurbinectedin in this single-arm study. Twenty-nine samples were available at baseline, and seven additional matched samples at day one of cycle two of treatment. Survival curves and rates between groups were compared using the log-rank test and Kaplan—Meier method. Statistical significance was set at P value <0.05.

Results: Updated median overall survival (OS) was slightly increased to 11.5 months [95% confidence interval (CI) 8.8-13.8 months]. Thirty-six patients (85%) had died. The OS rate at 12 and 18 months was 47% (95% CI 32.1% to 61.6%) and 31% (95% CI 17.8% to 45.0%), respectively. Median progression-free survival was 4.1 months (95% CI 2.6-5.5 months). No new safety signals were observed. Patients with lower frequencies of regulatory T cells, as well as lower tumor-associated macrophages (TAMs) at baseline, had a better OS. Comparing matched biopsies, a decrease of M2 macrophages was observed in five out of seven patients after exposure to lurbinectedin, and two out of four patients showed increased CD8+ T-cell infiltrates in tumor.

Discussion: Lurbinectedin continues to be active in patients with progressing malignant pleural mesothelioma. According to our very small sample size, we hypothesize that baseline TAMs and regulatory T cells are associated with survival. Lurbinectedin seems to inhibit conversion of TAMs to M2 phenotype in humans.

Key words: lurbinectedin, malignant pleural mesothelioma, regulatory T cells, tumor-associated macrophages, M2 phenotype, tumor-infiltrating lymphocytes

INTRODUCTION

The oncogenic transcription inhibitor lurbinectedin is being developed as a treatment for various cancers. According to the safety and efficacy data by Trigo et al.,[1] the drug has been granted orphan drug status for the treatment of small-cell lung cancer (SCLC) by regulatory authorities in multiple countries worldwide and was approved by the Food and Drug Administration in June 2020 for the treatment of metastatic SCLC with disease progression on or after platinum-based chemotherapy.[2]

Lurbinectedin exerts a dual function. It binds to the DNA of gene regulatory regions, thus, evicting oncogenic transcription factors and leading to apoptosis. Simultaneously it inhibits cytokine transcription of circulating monocytes and their accumulation in tumors and, therefore, may also have

*Correspondence to: Dr Michael Mark, Department of Oncology/Haematology, Kantonsspital Graubünden, Loestrasse 170, 7000 Chur, Switzerland. Tel: +41-812566646; Fax: +41-812566668
E-mail: michael.mark@ksgr.ch (M. Mark).

an immunomodulatory function.[3] Circulating monocytes can be converted to tumor-associated macrophages (TAMs), which play a key role in the cancer microenvironment and can influence tumor growth and progression.[4] Classically activated 'M1' phenotype macrophages driven by interferon-γ and bacterial products can lead to antitumor responses and cytotoxicity. By contrast, TAMs can be differentiated towards an immunosuppressive, tumor-promoting 'M2-like' phenotype driven by cytokines, such as colony-stimulating factor-1 (a monocyte attractant as well as a macrophage survival and polarization signal).[5] They also can promote the immunosuppressive activity of regulatory T cells (Tregs) through a bidirectional interaction stimulating macrophages to produce immunosuppressive cytokines such as interleukin 10 and transforming growth factor-β.[4,5] M2-TAM macrophages express high levels of CD206 (a mannose receptor with endocytosis and phagocytosis functions) which is associated with bad prognosis in many cancers.[6,7] In addition, M2-TAMs often express programmed death-ligand 1 (PD-L1) and PD-L2, which trigger the inhibitory programmed cell death protein 1 (PD-1)-mediated immune checkpoint in T cells.[8]

Preclinical models demonstrated that trabectedin, a lurbinectedin analogon, induces rapid apoptosis in mononuclear phagocytes by causing selective depletion of monocytes/macrophages with an associated reduction of angiogenesis, posing a key component of its antitumor activity.[9,10] These alterations of the inflammatory tumor microenvironment could also be shown with lurbinectedin *in vitro*, which selectively decreases the number of circulating monocytes and of macrophages and vessels in tumor.[3]

In malignant pleural mesothelioma (MPM) patients, a high number of CD8+ tumor-infiltrating lymphocytes (TILs) was suggested to be a good prognostic factor,[11] indicating that TILs could play a pivotal role in host antitumor response.

Our recently published clinical results of the SAKK 17/16 phase II trial showed promising efficacy of lurbinectedin as second- or third-line palliative therapy in MPM.[12] Here, we evaluated long-term outcome with approximately 17 additional months of follow-up. In addition, we analyzed the impact of lurbinectedin monotherapy on the tumor microenvironment at the cellular and molecular level to predict outcomes.

MATERIAL AND METHODS

The study population and procedures have already been described.[12] To perform this translational study, samples of 29 patients were available at initial diagnosis for translational analyses, and additional matched samples from 7 patients were gathered at day one of cycle two of treatment.

Hematoxylin–eosin staining and multispectral immunofluorescence staining

Hematoxylin–eosin (HE) and multiplex immunofluorescence (IF) stainings were carried out on 3.5-μm formalin-fixed paraffin-embedded samples as previously described.[13,14] HE slides were reviewed by a pathologist with confirmation of the tumor content and definition of the region of interest (JD). Multiplex IF staining was carried out on automated Ventana Discovery Ultra staining module (Ventana, Roche), with the following primary antibody-OPAL sequences: panel 1: 1st, mouse monoclonal anti-PD-1 (Biocare Medical, Pacheco, CA, ref ACI3137C)-OPAL570; 2nd, rabbit monoclonal anti-FOXP3 (Abcam, Cambridge, UK, ref ab99963)-OPAL520; 3rd, rabbit polyclonal anti-CD3 (Dako, Santa Clara, CA, ref A0452)-OPAL480; 4th, rabbit monoclonal anti-Calretinin (Ventana, 790-4467) or mouse monoclonal anti-WT1 (Ventana, 760-4397)-OPAL690; 5th, rabbit monoclonal anti-CD8 (Cellmarque, Rocklin, CA, ref 108R-16-RUO)-OPAL620; 6th, rabbit anti-CD20 (Dako, ref M0755)-OPAL780; panel 2: 1st, rabbit monoclonal anti-PD-L1 (Spring, Pleasanton, CA, ref M4420)-OPAL520; 2nd, mouse monoclonal anti-CD163 (Diagnostic BioSystems, Pleasanton, CA, ref Mob460)-OPAL620; 3rd, rabbit polyclonal anti-CD206 (Sigma, Merck & Cie Im Laternenacker 5, Schaffhausen, Switzerland, ref HPA004114)-OPAL570; 4th, rabbit monoclonal anti-CD68 (Dako, ref M0876)-OPAL480; 5th, rabbit monoclonal anti-Calretinin or mouse monoclonal anti-WT1 (as previously described)-OPAL690; 6th, rabbit monoclonal anti-CD8 (as previously described)-OPAL780. Nuclei were visualized by final incubation with Spectral DAPI (1/10, FP1490, Akoya Biosciences, Marlborough, MA). The slides were mounted with fluorescence mounting medium (ref S3023, Dako) and stored in the dark at 4°C until scanned and analyzed within 48 h.

Multispectral imaging and data analysis

Multiplex IF images were acquired on the Vectra® Polaris automated quantitative pathology imaging system (Akoya Biosciences, Marlborough, MA, USA), as described.[13,14] Quantification of the immune cells was carried out using the inForm active learning phenotyping algorithm by assigning the different cell phenotypes across several images representative of the whole scan. InForm software was trained to recognize cell phenotypes according to panel 1 and panel 2. This algorithm was then applied on the whole scan by batch to quantify all the different cell types. A homemade R-script was used to retrieve all combined phenotype cells and scoring in an output excel file.

Statistical analysis

In this study, as we do not know the levels of a given immune marker to be correlated with survival, we deliberately calculated the density of each target marker in a specific tissue area (stroma or tumor) for each patient and carried out: (i) comparison with time to survival periods (from 3 to 6 months, 6 to 12 months, 12 to 18 months, and >18 months, unpaired two-sample Wilcoxon tests) and (ii) stratification of each immune marker, generating a range of cut-off values spaced every 0.05 quantile (from 0.05 to 0.95, Supplementary Figure S1, available at https://doi.org/10.

Table 1. Patient characteristics of all patients ($N = 42$) and of the 29 patients available for translational analyses

Characteristics	FAS ($N = 42$)	Patients in TR analysis ($N = 29$)
Median age (range), years	68 (52-84)	69 (52-81)
Gender, *n* (%)		
Female	7 (16.7)	5 (17.2)
Male	35 (83.3)	24 (82.8)
ECOG performance status, *n* (%)		
0	20 (47.6)	14 (48.3)
1	22 (52.4)	15 (51.7)
Histology at initial diagnosis, *n* (%)s		
Epithelioid	33 (78.6)	24 (82.8)
Biphasic	4 (9.5)	3 (10.3)
Sarcomatoid	5 (11.9)	2 (6.9)
Previous immunotherapy, *n* (%)		
No	32 (76.2)	22 (75.9)
Yes	10 (23.8)	7 (24.1)
Time to progression on previous platinum-based chemotherapy, *n* (%)		
≥6 months	28 (66.7)	19 (65.5)
<6 months	14 (33.3)	10 (34.5)

ECOG, Eastern Cooperative Oncology Group; FAS, full analysis set; TR, translational research.

Table 2. Estimates of overall survival (%) using the Kaplan–Meier method at fixed time points 3-, 6-, 9-, 12-, and 18 months for the whole cohort and the subset of patients available for translational analyses

Months	FAS ($N = 42$)	Patients in TR analysis ($N = 29$)
3	95.2% (82.3% to 98.8%)	96.6% (77.9% to 99.5%)
6	73.8% (57.7% to 84.6%)	72.4% (52.3% to 85.1%)
9	64.3% (47.9% to 76.7%)	62.1% (42.1% to 76.9%)
12	47.6% (32.1% to 61.6%)	48.3% (29.5% to 64.8%)
18	31.0% (17.8% to 45.0%)	31.0% (15.6% to 47.9%)

FAS, full analysis set; TR, translational research.

1016/j.esmoop.2022.100446), to define immune marker candidates.

Directed significance is defined as the negative log of value multiplied by sign of the Cox regression coefficient (where value is the statistical significance of the Cox model estimated with the Wald test). This way, a scale of significance discriminating positive and negative correlation of a specific marker with the survival was obtained and should be considered exploratory and hypothesis generating.

Survival curves and rates between groups were compared using the log-rank test and Kaplan–Meier method at a specific time point, respectively.

Statistical significance was set at P value <0.05. No correction for multiple testing was applied, thus all analyses are considered exploratory and hypothesis generating. SAS 9.4 (SAS Institute Inc., Cary, NC) and R v3.5.1 (Foundation for Statistical Computing, Vienna, Austria) were used.

RESULTS

Patient outcomes

Overall, 42 patients were treated with lurbinectedin. Patient demographics, baseline disease characteristics, and primary efficacy results have been previously described.[12] Patient characteristics are shown in Table 1 and were similar between the whole cohort and the patients available for translational analyses.

At final data cut-off (22 March 2021) the median follow-up was 32.8 months [95% confidence interval (CI) 28.5-39.0 months]. Treatment had been discontinued in all patients. Thirty-six patients (85%) had died. Median overall survival (OS) of the 42 patients was 11.5 months (95% CI 8.8-13.8 months). The death causes were progression in 31 patients and viral pneumonitis, acute dyspnea, suicide, heart failure, and COVID-19 in one patient each. The OS rate at 12 months and 18 months was 47% (95% CI 32.1% to 61.6%) and 31% (95% CI 17.8% to 45.0%), respectively (Table 2). Median progression-free survival was 4.1 months (95% CI 2.6-5.5 months) with one patient being free from progression at 12 months. OS data of the 29 patients available for translational analyses showed no relevant difference compared with the whole cohort (Table 2). No new safety signals were observed with longer follow-up.

Translational research

The immune infiltrates distribution for the 29 available baseline samples are shown in Figure 1. Patients were classified in four groups according to their survival time with $n = 8$ for 3-6 months, $n = 7$ for 6-12 months, $n = 10$ for 12-18 months, and $n = 4$ for >18 months, to assess the immune markers associated with survival benefit. Patients with the lowest survival (3-6 months) had higher Tregs and M2 distribution in stroma and tumor at baseline compared with patients with >18 months survival (Figure 1A and B, respectively). Accordingly, Kaplan–Meier survival probabilities show improved survival outcome in patients with lower Tregs (Figure 2A and B) and lower M2-TAMs (Figure 2C and D). No significant differences were observed for other immune markers such as PD-1, PD-L1, CD8 cells, or M1 macrophages.

The immuno-IF staining images are shown for a representative patient (1716-017) for both panel 1 and panel 2 in Figure 3A and B, respectively. After lurbinectedin therapy, tumor samples were available for seven patients and were stained with the same immuno-IF panels. An example is shown for patient 1716-007 in Figure 3C and E (before treatment), and Figure 3D and F (after treatment). Lurbinectedin led to a preferential decrease of M2-TAMs (decrease of CD206 expression after treatment) in five out of seven patients (Figure 3G) whereas CD163 macrophage marker was generally not affected (Figure 3H). Accordingly, an increase of CD8+ T-cell infiltrates in tumor was observed in two out of four patients available (data not shown).

DISCUSSION

In this updated analysis of the SAKK 17/16 phase II trial, lurbinectedin continues to result in prolonged OS when administered in second- or third-line therapy in a subset of patients with advanced MPM. Almost half of the patients

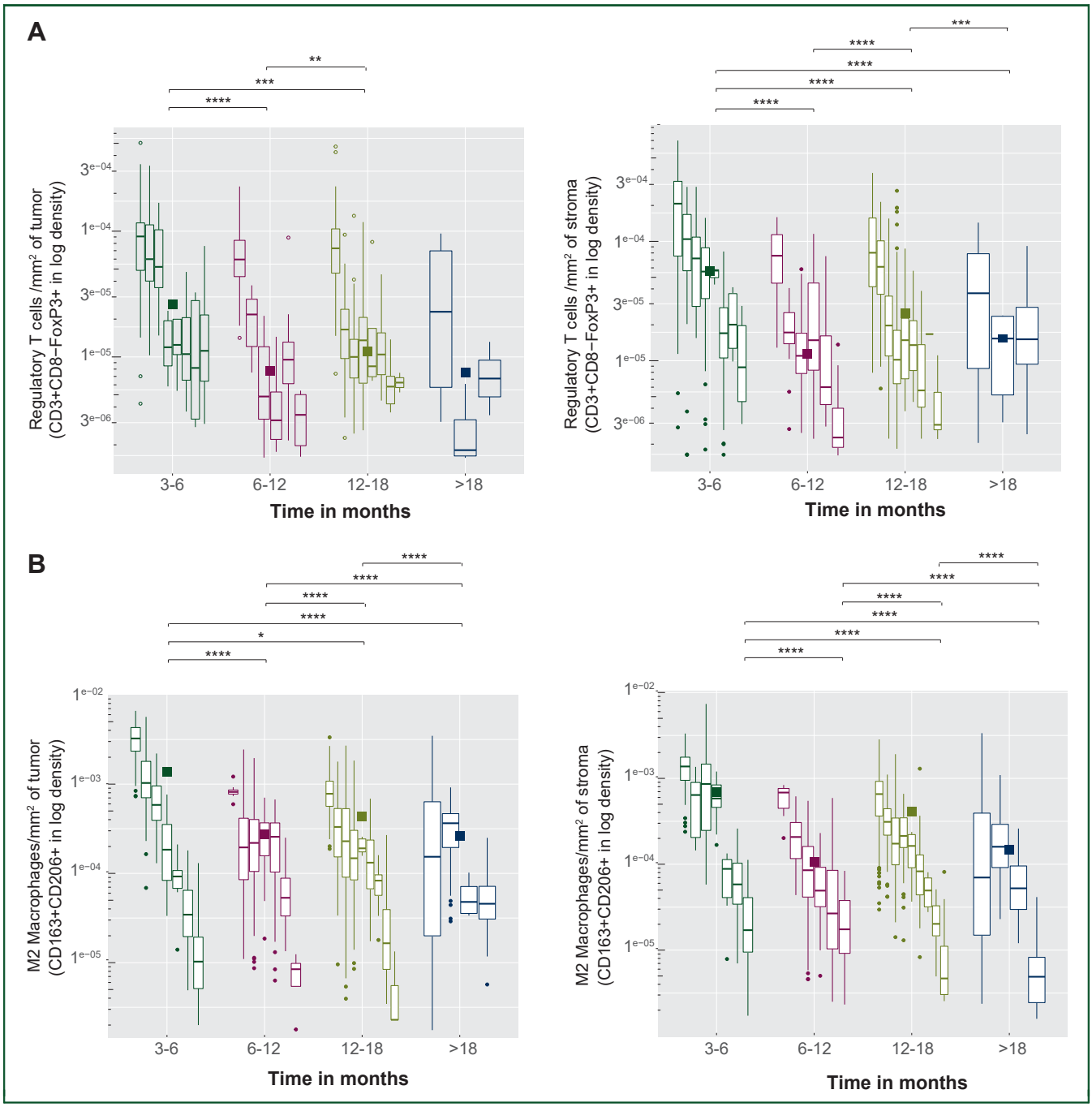

Figure 1. Baseline immune infiltrates quantification of patient's formalin-fixed paraffin-embedded samples according to their survival time ($n = 8$ for 3-6 months, $n = 7$ for 6-12 months, $n = 10$ for 12-18 months, and $n = 4$ for >18 months) shown in logarithmic scale, each row representing one patient. The frequencies of regulatory T cells [(A) CD3+CD8−FoxP3+], and M2 macrophages [(B) CD163+ CD206+] in tumor area (left panels) and peritumoral area (right panels) are shown for the different survival groups following lurbinectedin therapy. Unpaired two-sample Wilcoxon test: *$P < 0.005$; **$P < 0.001$; ***$P < 0.0001$; ****$P < 0.00001$.

(47%) had a median OS of ≥12 months, which compares favorably with historical trials showing OS of <9 months.[15-18] Importantly, we observed a clinically meaningful subgroup of patients (19%) who experience long-term benefit from lurbinectedin and continue to be alive ≥18 months. To further explore potential biologic mechanisms associated with prolonged survival with lurbinectedin treatment, we analyzed *in vivo* characteristics of the tumor and its microenvironment of these patients. We could demonstrate that in pretreatment tumor samples of patients with long-term survival (OS >18 months), less Treg cells and less tumor-promoting 'M2-like' TAMs were found in the tumor and peritumoral area compared with patients with shorter survival (OS <6 months) (Figures 1 and 2).

It has previously been demonstrated that M2-TAMs stimulate tumor progression and limit therapeutic responses by having strong immunosuppressive functions.[19-23] To date, the decrease of the number of tumor macrophages and circulating monocytes of lurbinectedin by inducing caspase-dependent apoptosis specifically in the

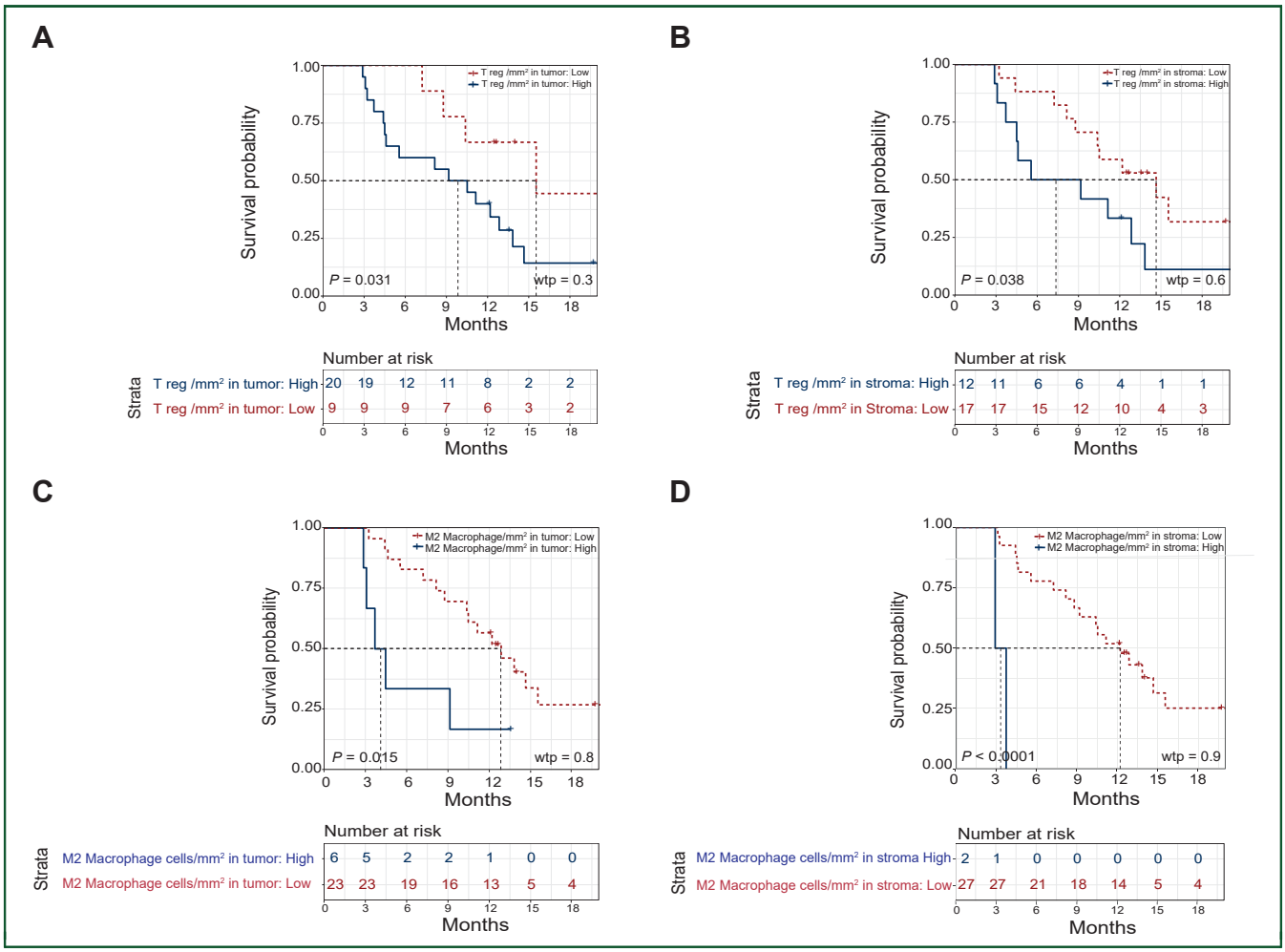

Figure 2. Kaplan–Meier survival probability curves are shown for regulatory T cells [(A) and (B) CD3+CD8−Foxp3+] and for M2 macrophages [(C) and (D) CD206+CD163+] in (A) and (C) tumor and in (B) and (D) peritumoral area according to the quantile shown in Supplementary Figure S1, available at https://doi.org/10.1016/j.esmoop.2022.100446. *N* = 29 patients at baseline; *P* and Wald test *P* (wtp) values are shown on the graph.

monocyte-macrophage lineage has only been shown in mouse tumor models.[3] Here, we present for the first time a decrease of the CD206 marker on M2 macrophages in patients treated with lurbinectedin (Figure 3), while CD163 remains stable, suggesting a preferential conversion of M2-TAMs into the M1 phenotype and/or inhibition of M2-TAM phenotype under lurbinectedin treatment. Furthermore, the observed increase of tumor CD8+ T cells in patients with better OS may have contributed to the clinical immunomodulatory effect of lurbinectedin, which could have further influenced the outcome of our patients. Nevertheless, the low numbers of patients does not allow any conclusions to be made regarding CD8+ T-cell infiltration and survival outcome.

The observation of lurbinectedin-induced reduction of M2-TAM density (observed with the decrease of CD206 expression in Figure 3) raises the question as to whether the combination of lurbinectedin and immune-checkpoint inhibitors (ICIs) could further improve the effectiveness of treatment. Accordingly, clinical trials investigating lurbinectedin in combination with ICIs, such as pembrolizumab, in relapsed SCLC (ClinicalTrials.gov Identifier: NCT04358237) are already recruiting and their results are eagerly awaited.

The major limitation of our study is the low number of patient tumor samples in the post-lurbinectedin setting. In addition, as baseline tumor samples had been obtained at diagnosis and not immediately before exposure to lurbinectedin, we cannot exclude that other factors could have influenced the observed immunomodulatory changes. We are aware that more data in this field are needed before the mentioned immune cells can be used to guide treatment. Our results, however, are biologically plausible given the known mechanism of action of lurbinectedin. Eventually, our observations could be of great clinical relevance if confirmed in a larger study given the heterogeneity of MPM and the current absence of predictive biomarkers to identify patients likely to have long-term benefit from treatment.

Conclusions

In summary, lurbinectedin continues to be active in patients with progressing MPM. TAMs and TILs are associated with

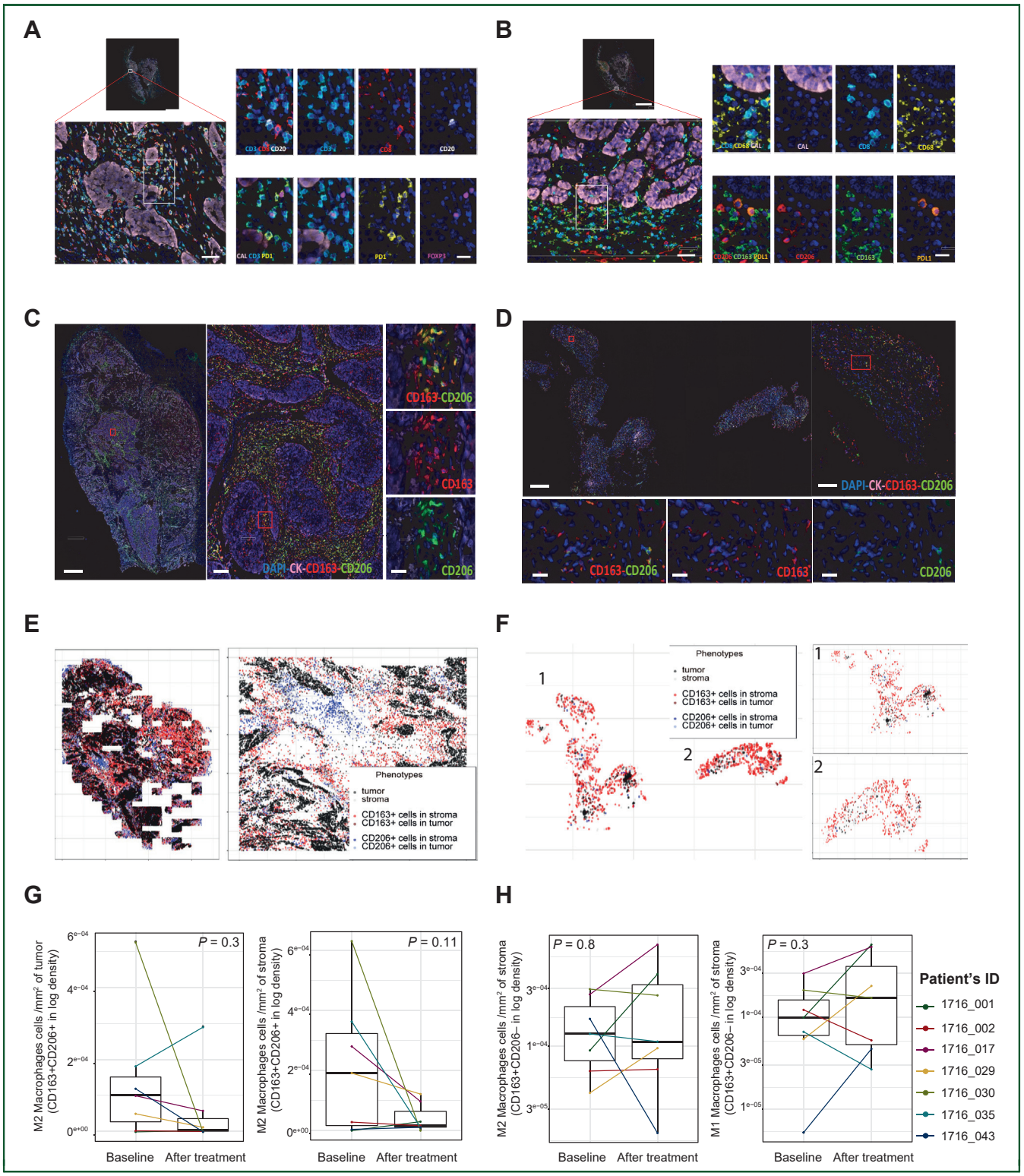

Figure 3. (A) (B) Representative multispectral immunofluorescence (IF) images of a patient are shown for panel 1 (A) and panel 2 (B) with highlights staining of T cells (CD3+, CD8+), B cells (CD20+), regulatory T cells (CD3+CD8−FOXP3+), immunoregulatory marker programmed cell death protein 1 and calretinin tumor marker for panel 1 (A, right panel) and T cells (CD8+), macrophages (CD68+, CD163+), mannose receptor (CD206), and immunoregulatory programmed death-ligand 1 marker for panel 2 (B, right panel). Scale bars: 5 mm (top left); 50 µm (bottom left), 20 µm (bottom right). (C) (D) Multispectral immune-IF images for mannose receptor CD206 [green or blue in (E), (F)], M1 macrophages CD163 (red), M2 macrophages (CD163+CD206+, yellow) and calretinin (pink) are shown for paired sample 1716_017 at baseline (C) and after treatment (D). Scale bars: (C): 3 mm (left), 50 µm (middle) and 20 µm (right); (D): 800 µm (left), 80 µm (middle), 20 µm (right). The IF images [(C), (D), left panels], as well as its pixel reconstruction [(E), (F), left panels] and its magnification [(E), (F), right panels] are shown. The decrease of M2 macrophages [(G) CD163+ CD206+] from baseline to after treatment are shown for the seven paired samples both in tumor (left panels) and peritumoral areas (right panels), whereas the M1 macrophages were not affected [(H) CD163+CD206−]. *P* values from unpaired two-sample Wilcoxon test are shown in the graph.

long-term survival, which can be used as prognostic and potentially as predictive markers for treatment with lurbinectedin. Further evaluation in a larger randomized trial is warranted.

ACKNOWLEDGEMENTS

This study was sponsored by the Schweizerische Arbeitsgemeinschaft für Klinische Krebsforschung (SAKK). We would like to thank Professor George Coukos for useful discussion and David Barras for his help with the code for stratification analysis.

FUNDING

This study was supported by PharmaMar (no grant number) and the Swiss State Secretariat for Education, Research and Innovation (SERI) (no grant number).

DISCLOSURE

MF declared unrestricted grants from Bristol Myers Squibb (BMS) and AstraZeneca paid to his institution, advisory board roles for AstraZeneca, Merck Sharp & Dohme (MSD); Roche, BMS; Boehringer Ingelheim, Pfizer, Takeda, payment for expert testimony from Takeda and Roche, meeting support from Merck, and participation on a Data Safety Monitoring Board for Roche.

FG declared outside the submitted work personal fees for advisory role, speaker engagements and travel and accommodation expenses from MSD, Novocure, BMS, Boehringer Ingelheim, Pharmamar, Novartis, and Pierre Fabre, outside the submitted work personal fees for advisory role, speaker engagements, and travel, and accommodation expenses from MSD, Novocure, BMS, Boehringer Ingelheim, Pharmamar, Novartis, and Pierre Fabre, outside the submitted work personal fees for advisory role, speaker engagements and travel and accommodation expenses from MSD, Novocure, BMS, Boehringer Ingelheim, Pharmamar, Novartis, and Pierre Fabre.

MP declared consulting fees from AbbVie, AstraZeneca, BMS, Boehringer Ingelheim, Esei, MSD, Novartis, Pfizer, Roche, Takeda, Merck, speakers fee from Janssen, payment for expert testimony from Takeda and Novartis, support for attending meetings and/or travel from AstraZeneca, BMS, Boehringer Ingelheim, Roche, Vifor, and Takeda.

PZ declared payment or honoraria for lectures, presentations, speakers bureaus, manuscript writing or educational events from MSD, Astellas, Janssen, Sanofi, Ipsen, Pfizer, Novartis, BMS, Amgen, AstraZeneca, Roche, and Bayer, support for attending meetings and/or travel from MSD, Astellas, Janssen, Sanofi, Ipsen, Pfizer, Novartis, BMS, Amgen, AstraZeneca, Roche, and Bayer, participation on a Data Safety Monitoring Board or Advisory Board for MSD, Astellas, Janssen, Sanofi, Ipsen, Pfizer, Novartis, BMS, Amgen, AstraZeneca, Roche, and Bayer.

GLC declared payment or honoraria for lectures, presentations, speakers bureaus, manuscript writing, or educational events from Novocure, Zai Lab, MSD Oncology, AstraZeneca, BMS, and Bayer, participation on a Data Safety Monitoring Board or Advisory Board for Novocure.

RvM declared advisory boards fees from AstraZeneca, MSD; Roche, Bristol-Myers Squibb; Pfizer, Pharmamar, Novartis, GlaxoSmithKline, Amgen, Gillead, and payment or honoraria for lectures, presentations, speakers bureaus, manuscript writing, or educational events from Vifor.

SS declared grants from AstraZeneca, BMS paid to her institution, support for attending meetings and/or travel from Boehringer Ingelheim, Takeda, MSD, and participation on a Data Safety Monitoring Board or Advisory Board for MSD, AstraZeneca, Boehringer Ingelheim paid to her institution.

YM declared consulting fees from Merck-Serono, BMS, Roche, Novartis, support for attending meetings and/or travel from PharmaMar, Merck, and participation on a Data Safety Monitoring Board or Advisory Board for Merck-Serono, BMS, Roche, Novartis, all paid to his institution.

All other authors have declared no conflicts of interest.

REFERENCES

1. Trigo J, Subbiah V, Besse B, et al. Lurbinectedin as second-line treatment for patients with small-cell lung cancer: a single-arm, open-label, phase 2 basket trial. *Lancet Oncol*. 2020;21(5):645-654.
2. Markham A. Lurbinectedin: first approval. *Drugs*. 2020;80(13):1345-1353.
3. Belgiovine C, Bello E, Liguori M, et al. Lurbinectedin reduces tumour-associated macrophages and the inflammatory tumour microenvironment in preclinical models. *Br J Cancer*. 2017;117:628-638.
4. Mantovani A, Marchesi F, Malesci A, Laghi L, Allavena P. Tumour-associated macrophages as treatment targets in oncology. *Nat Rev Clin Oncol*. 2017;14:399-416.
5. Noy R, Pollard JW. Tumor-associated macrophages: from mechanisms to therapy. *Immunity*. 2014;41:49-61.
6. Fan W, Yang X, Fang H, Tong X, Zhu L, Wang S. Identification of CD206 as a potential biomarker of cancer stem-like cells and therapeutic agent in liver cancer. *Oncol Lett*. 2019;18(3):3218-3226.
7. Xu ZJ, Gu Y, Wang CZ, et al. The M2 macrophage marker *CD206*: a novel prognostic indicator for acute myeloid leukemia. *Oncoimmunology*. 2019;9(1):1683347.
8. Kryczek I, Wei S, Zou L, et al. Cutting edge: induction of B7-H4 on APCs through IL-10: novel suppressive mode for regulatory T cells. *J Immunol*. 2006;177:40-44.
9. Germano G, Frapolli R, Belgiovine C, et al. Role of macrophage targeting in the antitumor activity of trabectedin. *Cancer Cell*. 2013;23:249-262.
10. Allavena P, Signorelli M, Chieppa M, et al. Anti-inflammatory properties of the novel antitumor agent yondelis (trabectedin): inhibition of macrophage differentiation and cytokine production. *Cancer Res*. 2005;65(7):2964-2971.
11. Yamada N, Oizumi S, Kikuchi E, et al. CD8+ tumor-infiltrating lymphocytes predict favorable prognosis in malignant pleural mesothelioma after resection. *Cancer Immunol Immunother*. 2010;59(10):1543-1549.
12. Metaxas Y, Früh M, Eboulet EI, et al. Lurbinectedin as second- or third-line palliative therapy in malignant pleural mesothelioma: an international, multi-centre, single-arm, phase II trial (SAKK 17/16). *Ann Oncol*. 2020;31(4):495-500.
13. Dangaj D, Bruand M, Grimm AJ, et al. Cooperation between constitutive and inducible chemokines enables T cell engraftment and immune attack in solid tumors. *Cancer Cell*. 2019;35(6):885-900.e10.
14. Herrera FG, Ronet C, Ochoa de Olza M, et al. Low-dose radiotherapy reverses tumor immune desertification and resistance to immunotherapy. *Cancer Discov*. 2021;12:108-133.
15. Gregorc V, Gaafar RM, Favaretto A, et al. NGR-hTNF in combination with best investigator choice in previously treated malignant pleural mesothelioma (NGR015): a randomised, double-blind, placebo-controlled phase 3 trial. *Lancet Oncol*. 2018;19:799-811.

16. Ceresoli GL, Zucali PA. Vinca alkaloids in the therapeutic management of malignant pleural mesothelioma. *Cancer Treat Rev*. 2015;41:853-858.
17. Zucali PA, Perrino M, Lorenzi E, et al. Vinorelbine in pemetrexed-pretreated patients with malignant pleural mesothelioma. *Lung Cancer*. 2014;84:265-270.
18. Kindler HL, van Meerbeeck JP. The role of gemcitabine in the treatment of malignant mesothelioma. *Semin Oncol*. 2002;29:70-76.
19. Kryczek I, Zou L, Rodriguez P, et al. B7-H4 expression identifies a novel suppressive macrophage population in human ovarian carcinoma. *J Exp Med*. 2006;203(4):871-881.
20. De Palma M, Lewis CE. Macrophage regulation of tumor responses to anticancer therapies. *Cancer Cell*. 2013;23(3):277-286.
21. Galluzzi L, Vacchelli E, Bravo-San Pedro JM, et al. Classification of current anticancer immunotherapies. *Oncotarget*. 2014;5(24):12472-12508.
22. Mantovani A, Allavena P. The interaction of anticancer therapies with tumor-associated macrophages. *J Exp Med*. 2015;212(4):435-445.
23. Belgiovine C, D'Incalci M, Allavena P, Frapolli R. Tumor-associated macrophages and anti-tumor therapies: complex links. *Cell Mol Life Sci*. 2016;73(13):2411-2424.